

Supporting Information

Extended Short-wavelength Infrared Photoluminescence and Photocurrent of Nonstoichiometric Silver Telluride Colloidal Nanocrystals

Gahyeon Kim, Dongsun Choi, So Young Eom, Haemin Song, and Kwang Seob Jeong*

Department of Chemistry, Korea University, Seoul 02841, Republic of Korea.

*e-mail: kwangsjeong@korea.ac.kr

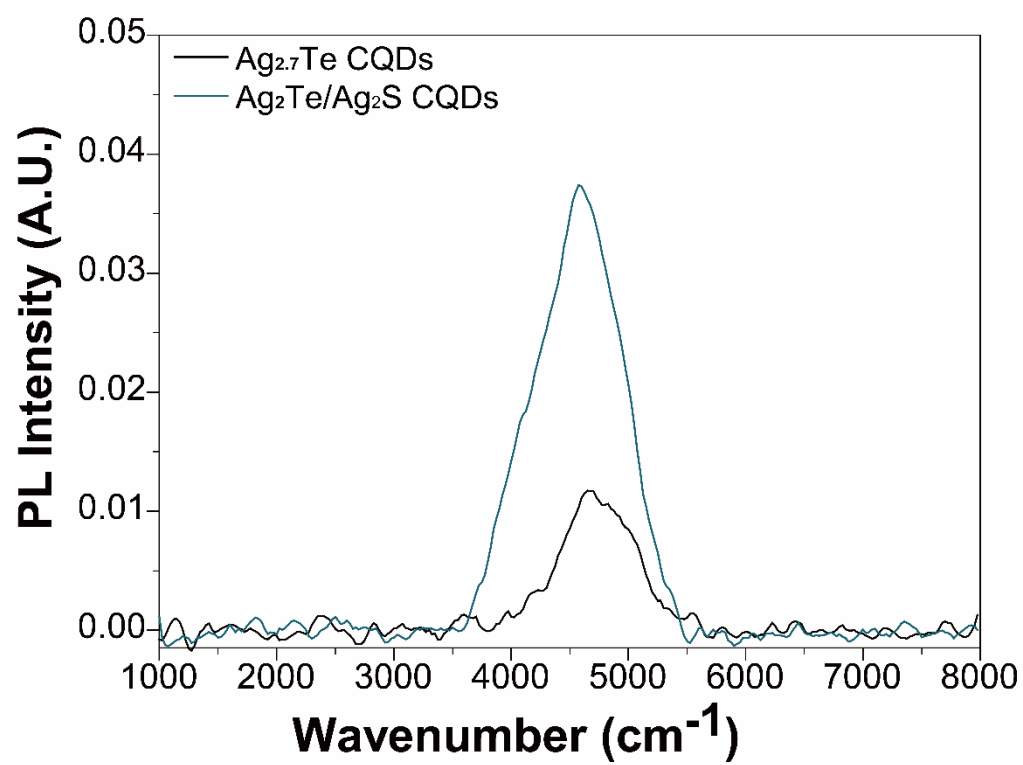


Figure S1. PL spectra of Ag_{2.7}Te CQDs and Ag₂Te/Ag₂S CQDs.

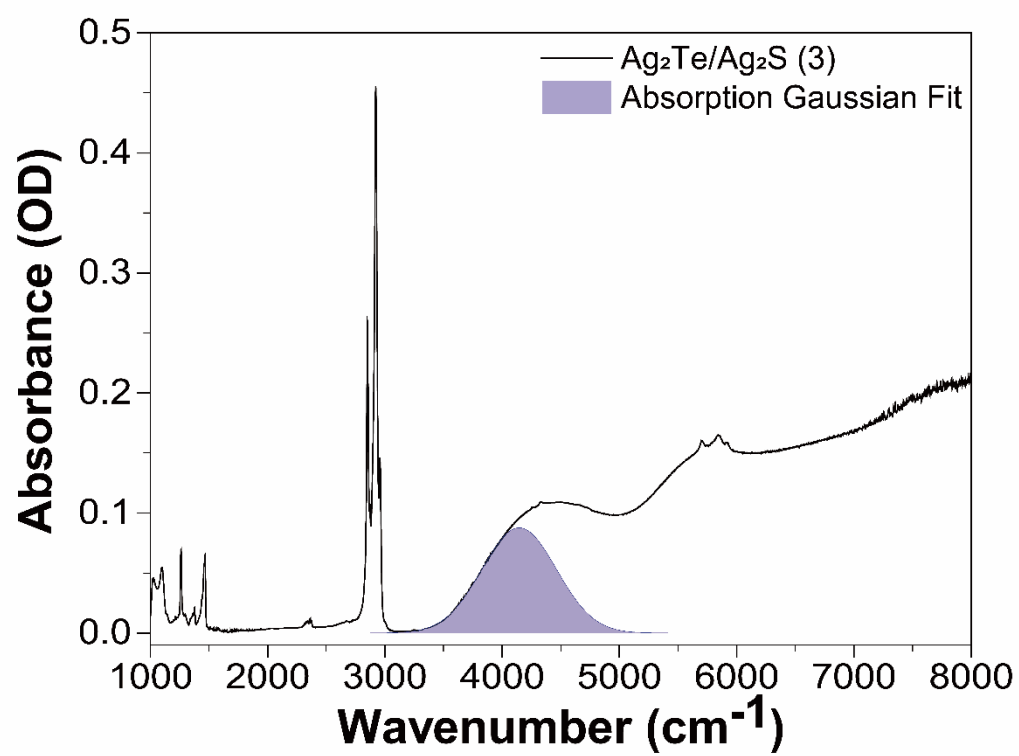


Figure S2. Absorption spectrum of $\text{Ag}_2\text{Te}/\text{Ag}_2\text{S}$ (3) with absorption Gaussian fit.

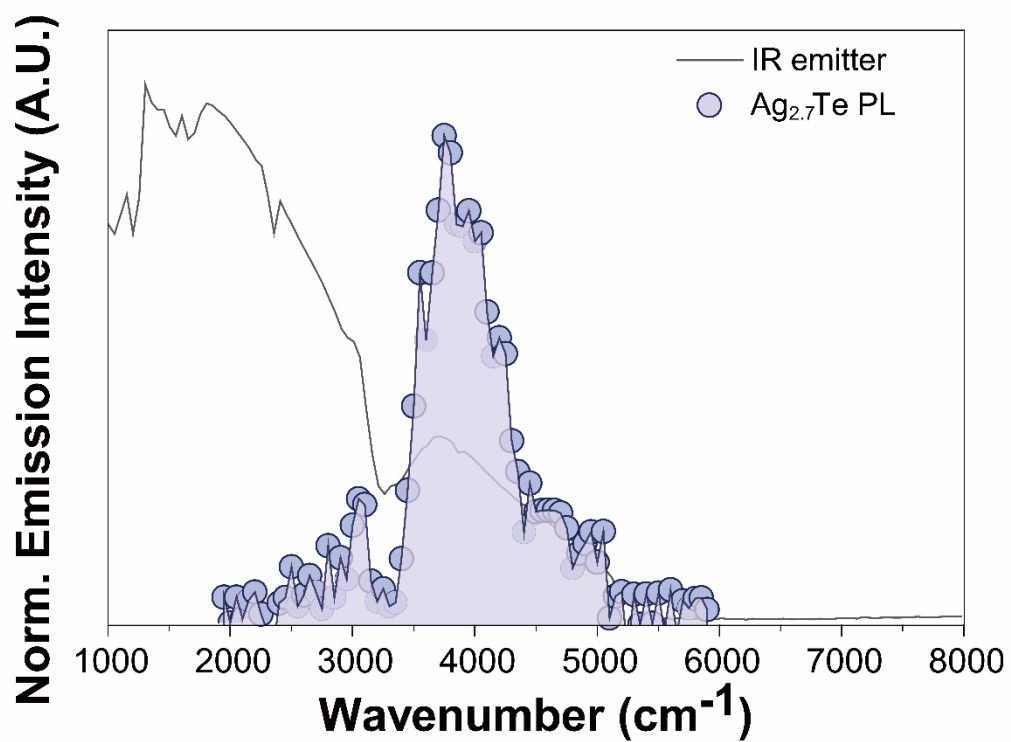


Figure S3. The PL spectrum of Ag_{2.7}Te QDs with the blackbody radiation of the IR global emitter.

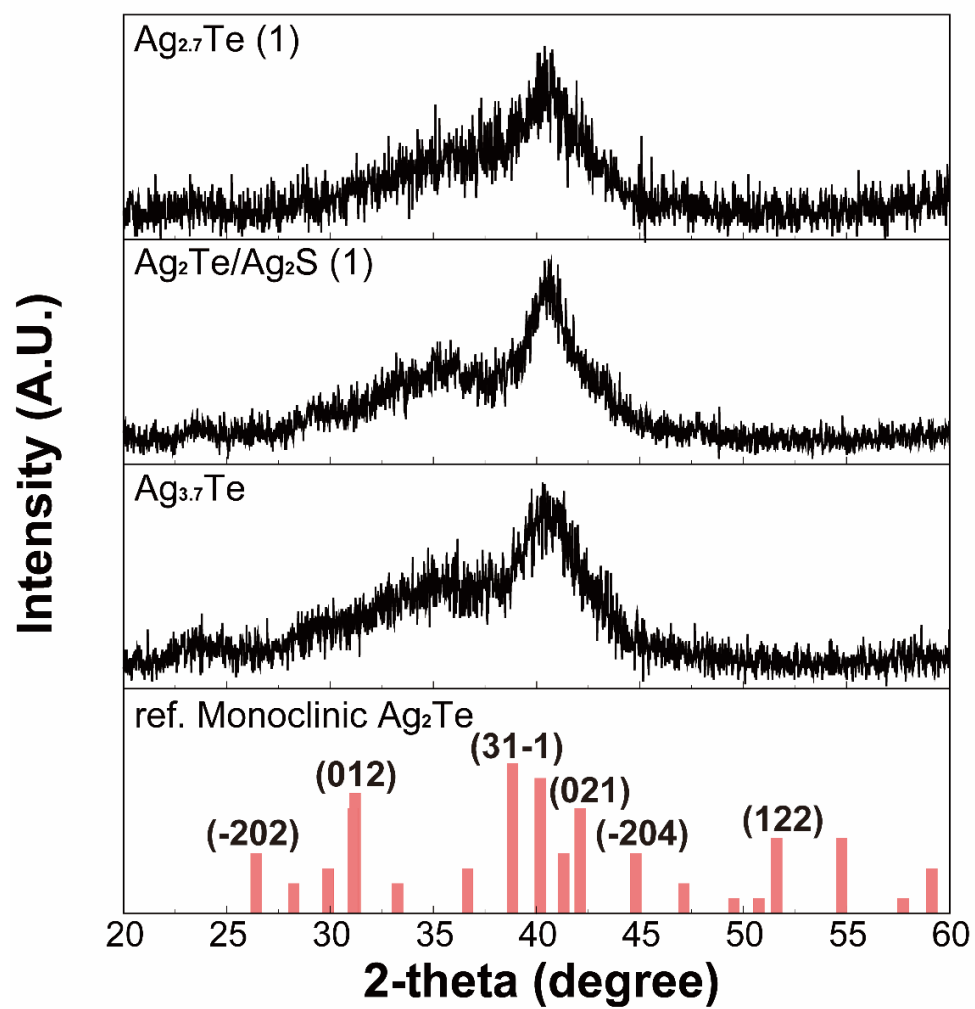


Figure S4. XRD spectra of $\text{Ag}_{2.7}\text{Te}$ (1), $\text{Ag}_2\text{Te}/\text{Ag}_2\text{S}$ (1), $\text{Ag}_{3.7}\text{Te}$ CQDs, and reference of monoclinic Ag_2Te .

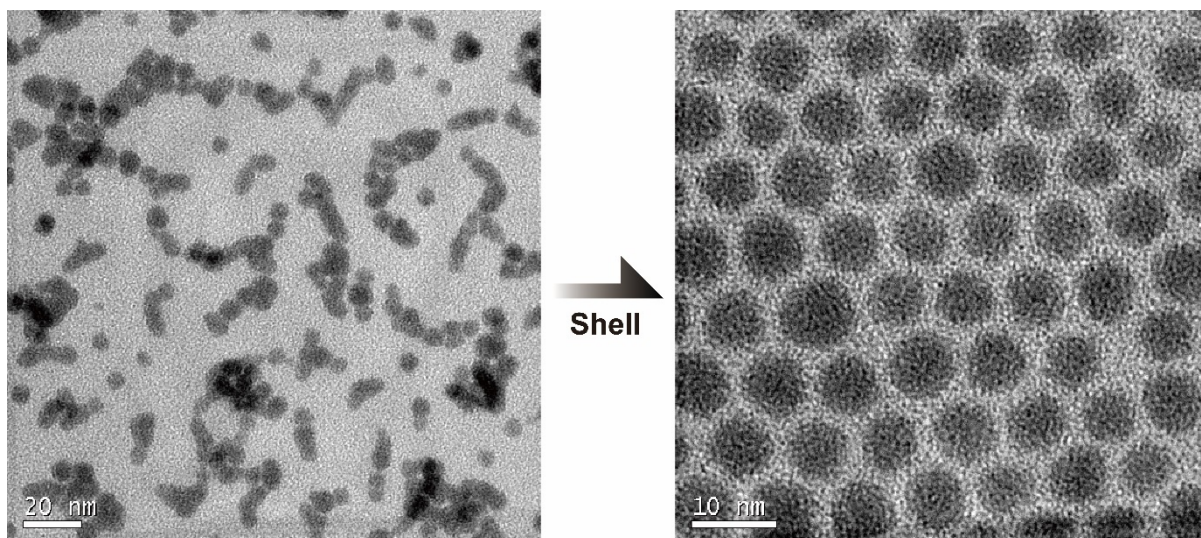


Figure S5. TEM images of Ag_{2.7}Te and Ag₂Te/Ag₂S QDs. By growing the Ag₂S shell, the deformation of crystal is significantly suppressed under e-beam irradiation.

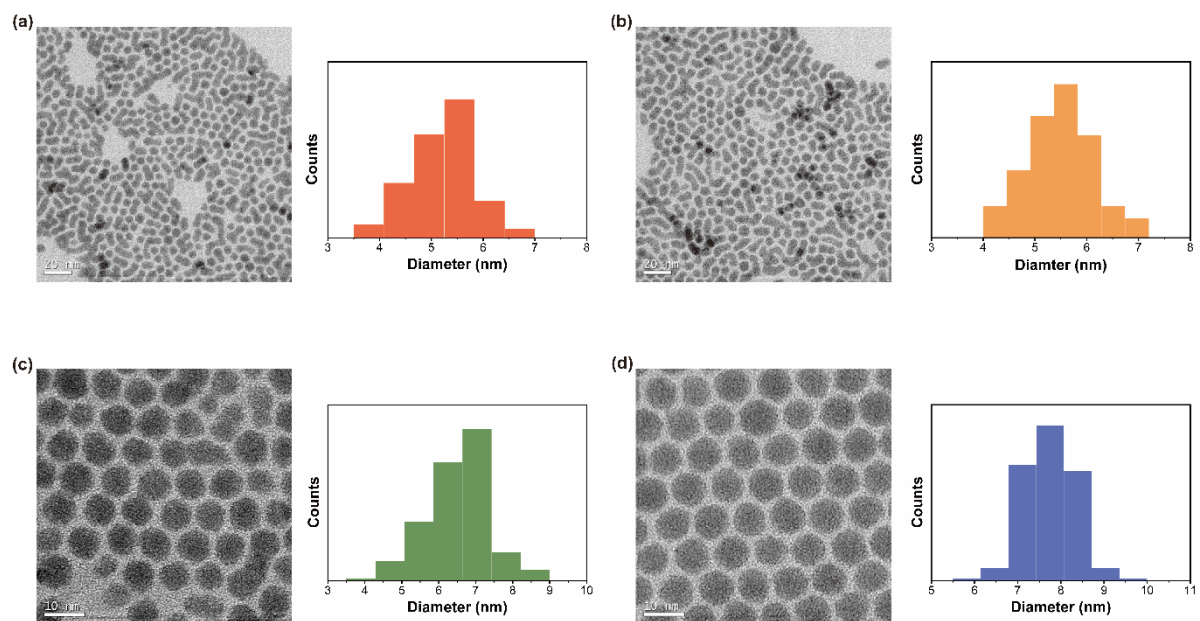


Figure S6. The TEM images of $\text{Ag}_2\text{Te}/\text{Ag}_2\text{S}$ QDs (1) 5.2 ± 0.6 nm, (2) 5.5 ± 0.7 nm, (3) 6.5 ± 0.8 , and #4 7.7 ± 0.6 .

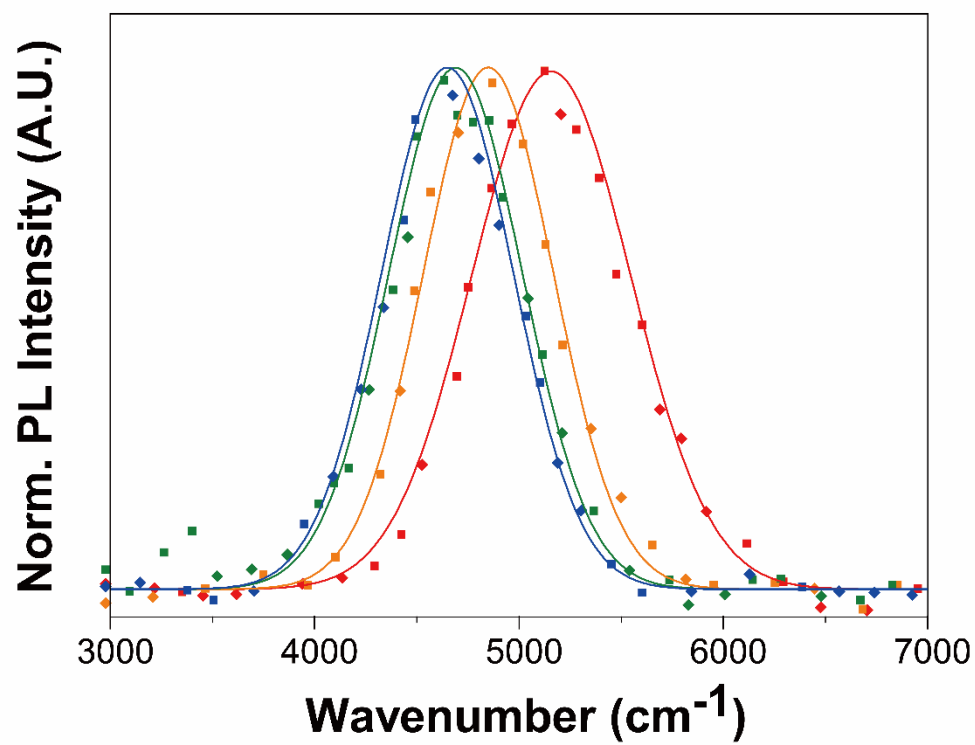


Figure S7. Normalized infrared photoluminescence spectra of Ag_{3.7}Te CQDs and corresponding Gaussian fit functions.

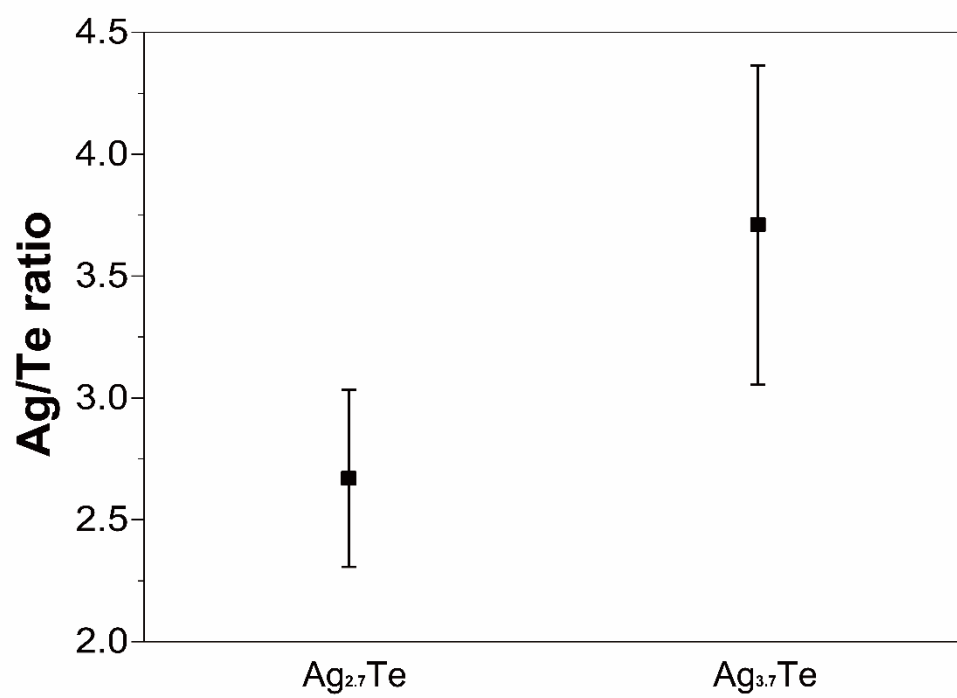


Figure S8. Ag/Te ratio of Ag_{2.7}Te and Ag_{3.7}Te CQDs.

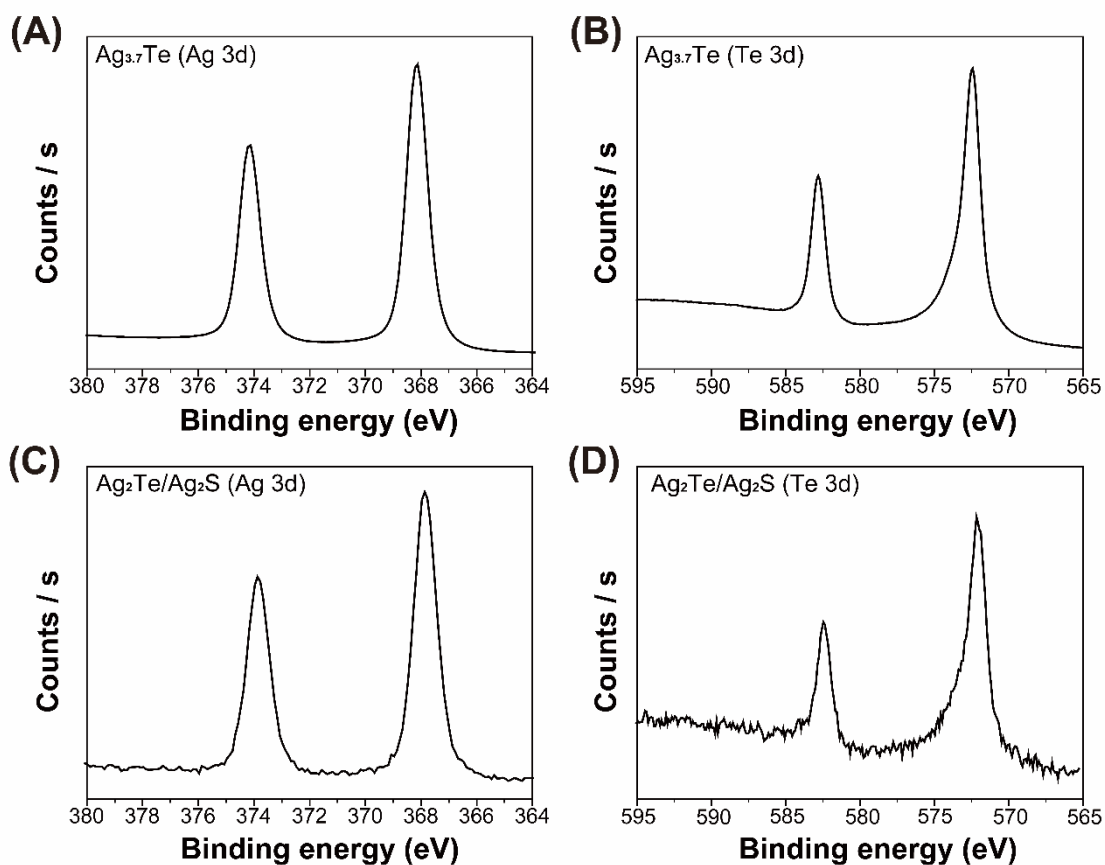


Figure S9. XPS spectra of (A) Silver 3d and (B) Tellurium 3d scan of $\text{Ag}_{3.7}\text{Te}$ QDs (C) Silver 3d and (D) Tellurium 3d scan of $\text{Ag}_2\text{Te}/\text{Ag}_2\text{S}$ QDs.

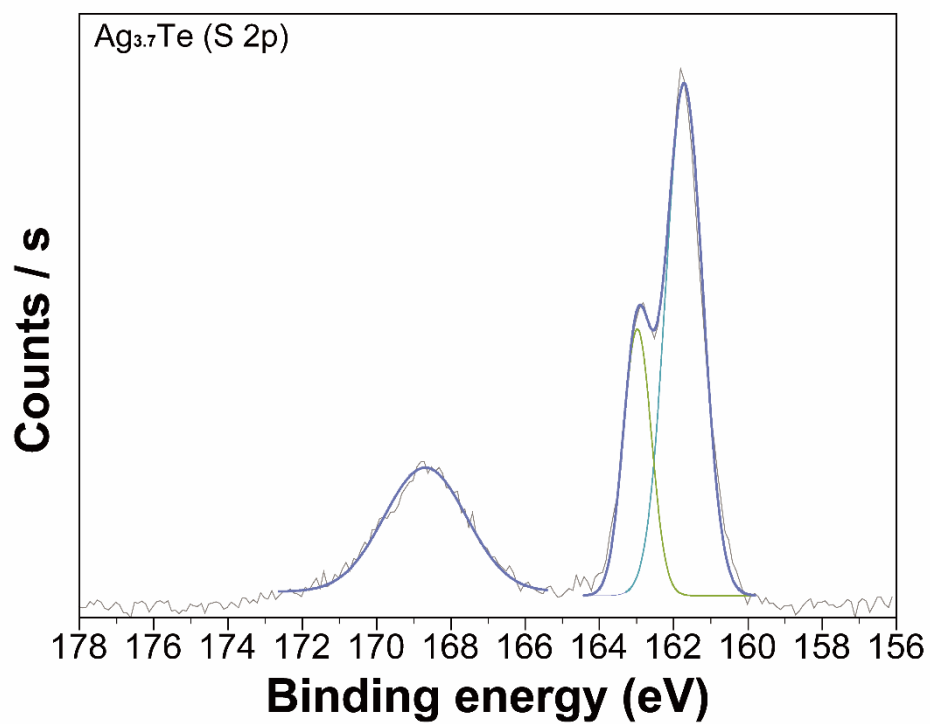


Figure S10. XPS spectrum of S 2p of Ag_{3.7}Te QDs with Gaussian fit functions.

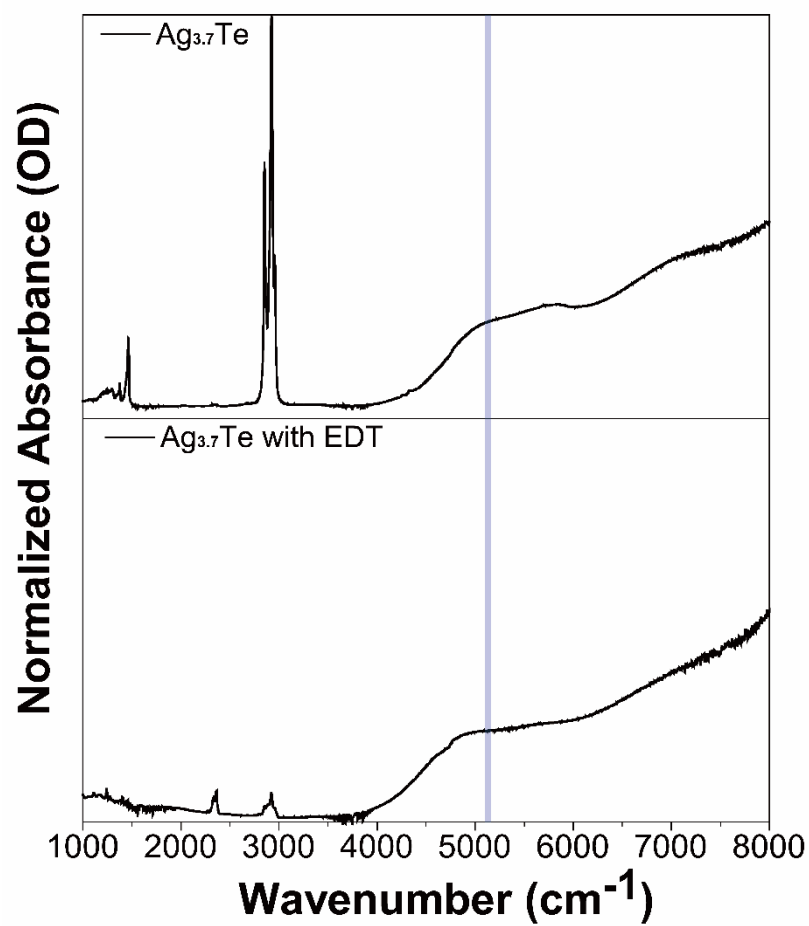


Figure S11. Absorption spectra of Ag_{3.7}Te QDs before and after exchange the ligand to ethanedithiol (EDT).

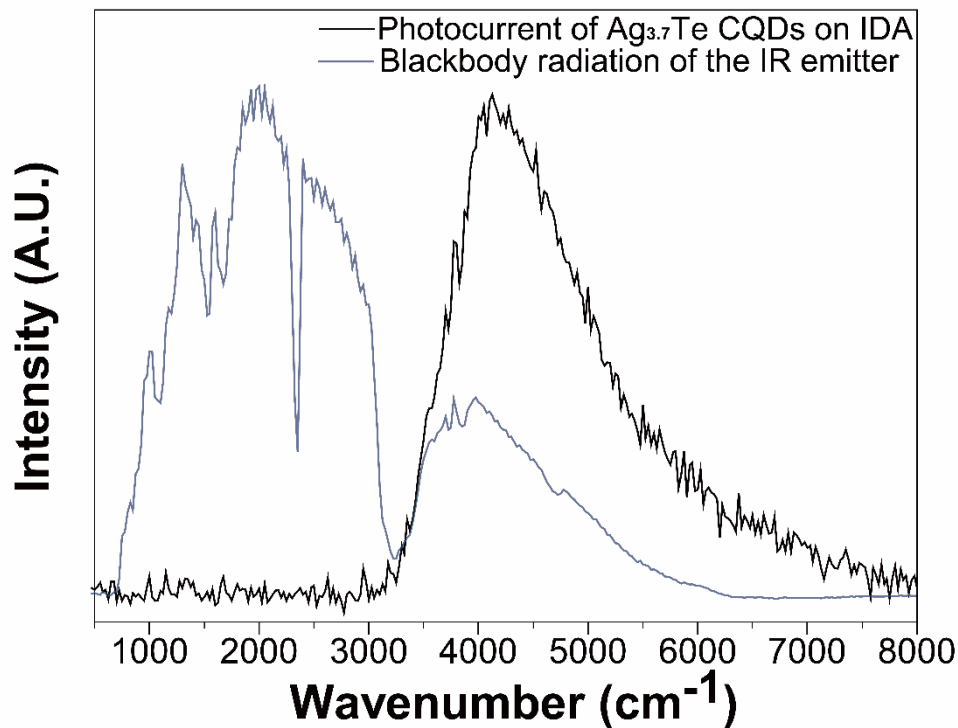


Figure S12. The infrared photocurrent spectrum of Ag_{3.7}Te CQDs on IDA electrode and the blackbody radiation of the IR emitter.

Figure S12 shows the comparison between the photocurrent spectra and the blackbody radiation of the IR emitter. At 6000-8000 cm⁻¹, the intensity of the blackbody radiation becomes weaker. Since the blackbody radiation attenuates at higher wavenumber, the spectrum in Fig. 4C follows the tail of the blackbody radiation spectra although the absorption feature of the Ag_{3.7}Te continuously increases with an increase of the frequency.